

EPCFormer: Expression Prompt Collaboration Transformer for Universal Referring Video Object Segmentation

Jiajun Chen^{1,2}, Jiacheng Lin³, Zhiqiang Xiao³, Haolong Fu³, Ke Nai⁴, Kailun Yang^{1,2,*}, and Zhiyong Li^{1,2,3,*}

Abstract—Audio-guided Video Object Segmentation (A-VOS) and Referring Video Object Segmentation (R-VOS) are two highly-related tasks, which both aim to segment specific objects from video sequences according to user-provided expression prompts. However, due to the challenges in modeling representations for different modalities, contemporary methods struggle to strike a balance between interaction flexibility and high-precision localization and segmentation. In this paper, we address this problem from two perspectives: the alignment representation of audio and text and the deep interaction among audio, text, and visual features. First, we propose a universal architecture, the Expression Prompt Collaboration Transformer, herein EPCFormer. Next, we propose an Expression Alignment (EA) mechanism for audio and text expressions. By introducing contrastive learning for audio and text expressions, the proposed EPCFormer realizes comprehension of the semantic equivalence between audio and text expressions denoting the same objects. Then, to facilitate deep interactions among audio, text, and video features, we introduce an Expression-Visual Attention (EVA) mechanism. The knowledge of video object segmentation in terms of the expression prompts can seamlessly transfer between the two tasks by deeply exploring complementary cues between text and audio. Experiments on well-recognized benchmarks demonstrate that our universal EPCFormer attains state-of-the-art results on both tasks. The source code of EPCFormer will be made publicly available at <https://github.com/lab206/EPCFormer>.

Index Terms—Referring video object segmentation, expression-visual attention, expression contrastive learning, multi-task learning, vision transformer.

I. INTRODUCTION

AUDIO-GUIDED video object segmentation (A-VOS) [1] and referring video object segmentation (R-VOS) [2]–[5] are two promising tasks, which aim to segment specific objects from video sequences by a given audio or text referring expression, facilitate a wide range of applications, such as video analysis and editing [6], human-computer interaction [7], and augmented reality [8]. Currently, both tasks have been widely discussed in various research fields, such as expression-video fusion [1], [9], [10], encoder-decoder

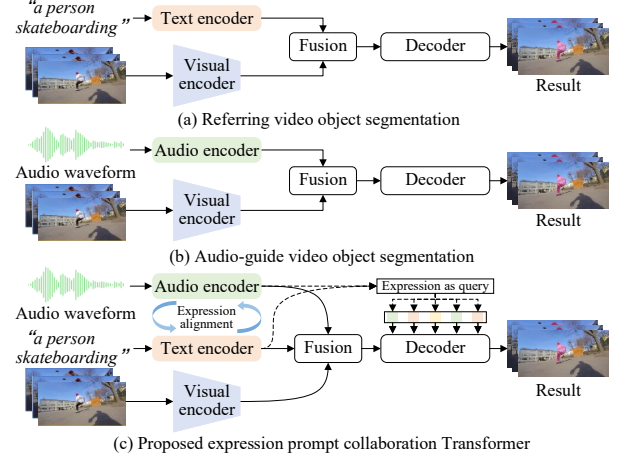


Fig. 1. Comparison of the proposed EPCFormer and existing methods. (a) A typical text-guided model for Referring Video Object Segmentation (R-VOS). (b) A typical audio-guided model for Audio-guided Video Object Segmentation (A-VOS). (c) Our proposed EPCFormer for universal referring video object segmentation, which is capable of processing both text- and audio-referring expressions.

architecture design [2], [3], and referring localization [11], [12], leading to significant advancements.

R-VOS is shown in Fig. 1(a), which has been widely studied due to its high accuracy and robust localization capabilities. Yet, the recent work [1] suggests that R-VOS may not be sufficiently efficient for practical applications. Notoriously, obtaining text clues in many real-world scenarios is difficult, whereas using voice aligns better with human-computer interaction use cases. In light of these factors, recent works [1], [13] attempt to use an Automatic Speech Recognition (ASR) model [14], [15] to transcribe audio expressions for R-VOS methods. Despite their progress, it is challenging for these methods to achieve optimal results due to inevitable translation errors and redundant computation parameters. To address these issues, the work of [1] proposes an A-VOS paradigm, as shown in Fig. 1(b), which directly fuses the audio and visual features to segment the referred object in the video. Although its interaction has some flexibility, it still faces challenges, such as extracting audio and aligning audio-visual features, leading to imprecise results in referred object localization. Nonetheless, audio- and text-guided methods manifest unique strengths. For example, precise textual description can alleviate audio semantic comprehension problems caused by ambiguous accents, varying emotions, and unstable speech speed. In addition, the

¹J. Chen, K. Yang, and Z. Li are with the School of Robotics, Hunan University, Changsha 410012, China.

²J. Chen, K. Yang, and Z. Li are also with the National Engineering Research Center of Robot Visual Perception and Control Technology, Hunan University, Changsha 410082, China.

³J. Lin, Z. Xiao, H. Fu, and Z. Li are with the College of Computer Science and Electronic Engineering, Hunan University, Changsha 410082, China.

⁴K. Nai is with the School of Computer and Communication Engineering, Changsha University of Science and Technology, Changsha 410114, China.

*Corresponding authors: Kailun Yang and Zhiyong Li. (E-mail: kailun.yang@hnu.edu.cn, zhiyong.li@hnu.edu.cn.)

emphasis provided by pronunciation serves as an effective cue for matching entities, attributes, or relations in the text. Therefore, a holistic and better understanding of the referring expressions can be gained from a deep integration of referring features from both modalities.

To address the challenges above, we introduce a novel universal architecture, Expression Prompt Collaboration Transformer (EPCFormer), and investigate its potential to learn and process text- and audio-referring expressions simultaneously. On the one hand, the features from one modality can be refined based on the knowledge learned from another modality, and vice versa, enhancing the overall integration and comprehension of the multi-modal data. To promote learning of the model and narrow the gap when processing these two modalities, we bridge audio and text domains via an efficient supervision mechanism based on contrastive learning, termed Expression Alignment (EA). Through a linear mapping layer, audio and text features are projected into a multi-modal embedding space, where referring semantics are aggregated. In this way, since deep-level audio and text features are well-aligned, the model better understands the semantic equivalence between audio and text expressions depicting the same objects.

On the other hand, an Expression-Visual Attention (EVA) mechanism, which comprises an Expression-Visual Interaction (EVI) module and an Audio-Text Collaboration (ATC) module, is designed to implement composable interactions among three types of modalities within a unified network. It assists the model in handling single audio, single text, or combined audio-text expressions in a unified manner. As shown in Fig. 1(c), our proposed model has two parallel process pathways. One pathway processes audio expressions, while the other one processes text expressions. Under the designed multi-task training, two types of referring features are densely integrated. Thus, the model is encouraged to learn a united multi-modal representation for visual and two types of referring features. In this way, the model effectively emphasizes matching features of visual regions and crucial elements of the referring expressions while establishing complementary connections between audio and text features. Experimental results from seven benchmarks, including Audio-Guided-VOS [1], Ref-YouTube-VOS [16], A2D-Sentence [2], and J-HMDB-Sentence [2], demonstrate our proposed EPCFormer achieves better or comparable results against state-of-the-art methods.

At a glance, this work delivers the following contributions:

- 1) We propose a universal architecture, Expression Prompt Collaboration Transformer (EPCFormer), for R-VOS and A-VOS. EPCFormer leverages audio and text as prompts to effectively segment the referred objects in videos, thus having high localization accuracy and exceptional convenience.
- 2) We propose an expression alignment mechanism that promises effective semantic-level contrastive learning between audio and text features and narrows the gap when processing these two modalities.
- 3) We propose an EVA module, including an EVI and ATC, to empower the model to handle interactions between features from text or audio cues and video, either independently or jointly, and establish complementary connections between audio and text features.

The subsequent sections of this paper are organized as follows: Sec. II provides a brief overview of related work. The proposed methods are described in detail in Sec. III. Experimental results are presented and discussed in Sec. IV, followed by the conclusion in Sec. V.

II. RELATED WORK

A. Referring Video Object Segmentation

R-VOS refers to segmenting specific objects from video frames based on the given text descriptions. Gavriluyuk *et al.* [2] first explore R-VOS and propose to encode linguistic clues as dynamic filters for visual features. To handle complex sentences, subsequent works widely adopt cross-modal attention mechanisms. For example, Wang *et al.* [10] employs an asymmetric cross-modal attention mechanism to mitigate linguistic variation. Ning *et al.* [17] introduce polar positional encoding and polar attention module to enhance the representation of positional relations in the referring text. In addition to multi-modal representation, some works explore incorporating temporal cues for boosting performance. For example, Ye *et al.* [18] propose a cross-frame self-attention module to capture the temporal context in consecutive frames. Ding *et al.* [19] adopt a dual-stream architecture to highlight the spatial-temporal features in multiple frames.

Recently, transformer-based methods have been used in R-VOS tasks. For example, Ding *et al.* [9] employ referring text to generate dynamic queries. Drawing inspiration from [20]–[22], MTTR [3] employs an instance-level segmentation transformer to process multimodal features and selects the optimal prediction for the referent object. With a similar pipeline, ReferFormer [23] leverages the linguistic expressions as decoder queries to attend to relevant regions in video frames. Some other works propose special language usage. For example, Gao *et al.* [4] interact visual features with different syntactic components to effectively harness textual cues. Most recently, Wu *et al.* [24] design a cross-frame query propagation to transform matching instance queries into subsequent frames.

In prior works, a common aspect is that their dynamic filter or attention-based approaches are limited to processing textual expressions. Therefore, the previous R-VOS paradigms hinder the applications in specific scenarios that only allow interaction via audio, *e.g.*, autonomous driving, and service robotics. Unlike existing methods, our proposed universal model can handle both text and speech for a broader range of applications. Additionally, our attention mechanism ensures that three different modalities, *i.e.*, audio, text, and visual, achieve effective interactions and complementary information exchange between two different referring expressions.

B. Audio-Guided Video Object Segmentation

A-VOS aims to predict a sequence of segmentation masks according to given audio expressions. Pan *et al.* [1] pioneer this task and leverage a transformer model with an audio-visual cross-modal attention mechanism to capture the intricate semantic representations of audio-video interactions. In addition to A-VOS, recent works predominantly center around audio-visual segmentation (AVS), proposed in [25], and segments

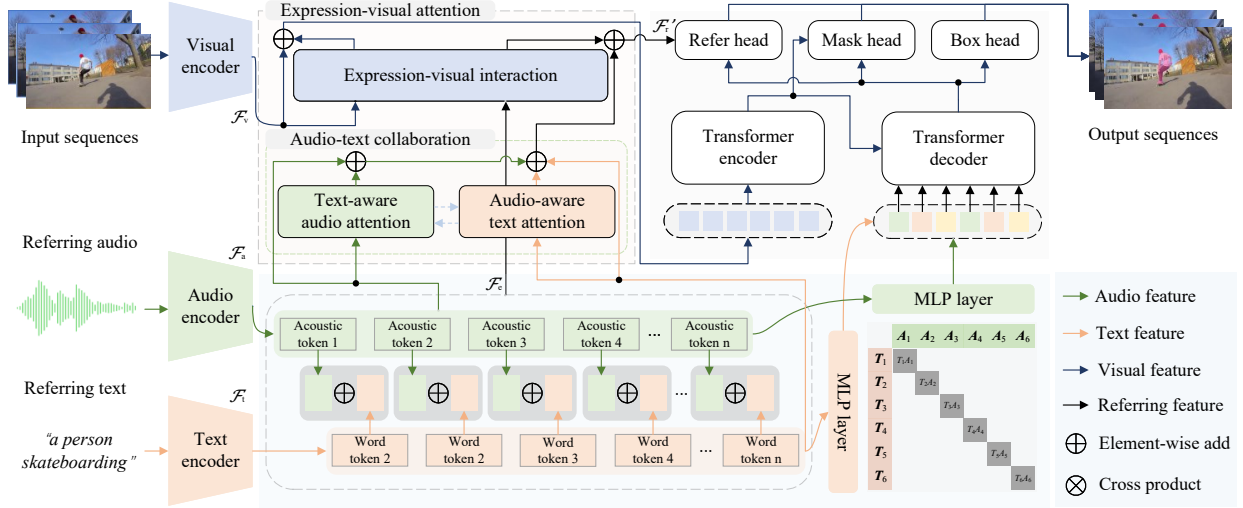


Fig. 2. An illustration of the proposed ECPFormer. Its components consist of four key stages: (1) multi-modal encoding, (2) expression alignment, (3) multi-modal interaction, and (4) segmentation and optimization.

sounding objects corresponding to the given sound. Similar to [1], Zhou *et al.* [25] utilize cross-modal attention to perform information exchange between visual and acoustic features. Afterward, following [20], [26], Gao *et al.* [27] employ the audio signals as queries for transformers to focus on distinctive features of sounding objects.

Despite the pioneering success of [1], existing methods are not efficient enough to model the semantic representations of audio-visual interaction contents. Concretely, the entire audio feature is injected into the visual feature, and the key phonetic units may not be effectively emphasized. Besides, while there is some excellent progress in AVS, the significant differences prevent these methods from being applied in A-VOS. In this work, audio cues are encoded by an improved pre-trained speech model to extract dense vectors for representation space and capture key semantic relationships.

C. Universal Visual Segmentation

Universal visual segmentation aims to unify multiple segmentation tasks into a single network [26], [28]–[33]. Through a shared backbone model, universal knowledge transfer between tasks becomes effortlessly attainable [34], [35]. Previously, to unify instance-, semantic-, and panoptic segmentation tasks, K-Net [36] employs a group of dynamic learnable kernels, whereas Mask2Former [26] builds on [37] and enhances its performance across different segmentation tasks by introducing learnable queries and a masked cross-attention mechanism. MCN [38] achieves collaborative learning of referring expression comprehension and segmentation. OneFormer [28] handles different segmentation predictions with a task-conditioned joint training strategy using a unified set of object queries for guidance. MaskDINO [39] aims to unify segmentation and detection, whereas OpenSeeD [40] jointly learns an open-vocabulary model for both tasks. Pix2SeqV2 [35] employs a shared pixel-to-sequence interface to handle four visual tasks. To achieve a more comprehensive model, some other works have recently transformed task-specific preconditions

into prompts. For example, UNINEXT [41] designs a prompt generation paradigm to handle ten instance perception tasks, including R-VOS, simultaneously. SAM [42] performs image segmentation with various user interactions through prompts. Similarly, SEEM [43] supports visual cues and combines multiple cues for promptable and interactive segmentation.

R-VOS and A-VOS are closely related due to their nature. Furthermore, texts offer more precise localization information, whereas audio extends the model’s applicability with an emphasis on keywords. Unfortunately, existing works lack an effective representation mechanism to integrate these two tasks. This paper presents a universal architecture and a joint training approach to handle R-VOS and A-VOS simultaneously, enabling the model to learn a cohesive representation space for audio and text expressions. Additionally, we propose audio-text contrastive learning to align features of different modality-referring expressions related to the same object, maximizing their similarity within the representation space. In this manner, the model can seamlessly transfer the multi-task learning knowledge to both tasks.

III. METHOD

A. Overview

The overview of our proposed ECPFormer is shown in Fig. 2, which consists of four major components: 1) **Multi-modal encoding** refers to extracting individual feature embeddings from audio, text expressions, and video sequences. 2) **Expression alignment** is to align the semantic-level representations of audio and text expressions before their deep interactions. 3) **Multi-modal interaction** is to achieve comprehensive and deep fusion among the three modalities before feeding them into the segmentation network. 4) **Segmentation and optimization** refers to feeding the obtained multi-modal features into a segmentation network to generate the masks. More details are presented in the following sections.

B. Multi-modal Encoding

Visual Encoder. Given a video sequence $\mathcal{I} = \{I_i\}_{i=1}^T$ with T frames, where $I_i \in \mathbb{R}^{3 \times H \times W}$ and i is the i^{th} frame in the video, following [21], [41], we investigate two main visual backbones, including ResNet-50 [44] and ViT-Huge [45], to extract visual features $\mathcal{F}_v \in \mathbb{R}^{C \times L_v}$ for each frame.

Text Encoder. Given a referring text clue $\mathcal{T} \in \mathbb{R}^N$ with N words, following [3], [23], a popular language model, namely BERT [46], is selected as text encoder to extract referring text features $\mathcal{F}_t \in \mathbb{R}^{C \times L_t}$.

Audio Encoder. As mentioned above, the existing method [1] encounters difficulties in extracting speech features and aligning them with visual features. Specifically, during the process of extracting raw acoustic features following [47], the network fails to extract the necessary crucial features in a learnable manner. All the information, including noise, in the audio, is indiscriminately fed into the network, leading to undesirable inductive biases and imprecise results of referred object localization. Accordingly, given a referring audio $\mathcal{A} \in \mathbb{R}^S$ with S samples, with the designed shallow layers, we extend the transformer-based HuBERT [15] pre-trained on large amounts of unlabelled data to extract hidden units acoustic embeddings $\mathcal{F}_a \in \mathbb{R}^{C \times L_a}$. On the one hand, unifying the features dimensions C of different categories of expressions facilitates subsequent joint processing of both modalities. On the other hand, by fine-tuning the learnable pre-trained backbone, we efficiently extract crucial features from the speech cues.

C. Expression Alignment

Given the inherent disparities between audio and text modalities, it is imperative to align these two modalities to alleviate the challenges associated with achieving complementarity between them. However, the presence of similar and diverse expressions brings significant challenges. Given a video frame I , which includes N_O objects $\mathcal{O} = \{O_i\}_{i=1}^{N_O}$, every object can be referred by N_T different text expressions $\mathcal{T}_i = \{T_{i,j}\}_{j=1}^{N_T}$ and N_A different audio expressions $\mathcal{A}_i = \{A_{i,k}\}_{k=1}^{N_A}$, where i is the i^{th} object, j is the j^{th} audio expression and k is the k^{th} text expression. We can obtain a relational mapping function, denoted as $\text{Seg}(I, T_{i,j}) = O_i$ and $\text{Seg}(I, A_{i,k}) = O_i$. As long as the textual and auditory expressions share the same meaning, both unambiguously refer to the same object, and consequently, the generated masks should be identical. Hence, it is crucial to ensure that feature vectors representing text and audio with the same meaning exhibit high similarity in the representation space. In this way, the proposed model can recognize that distinct types of expressions denoting the same semantics can refer to the same object.

Expression Contrastive Learning. Motivated by the insight, we integrate contrastive learning to supervise audio and text expressions. In contrast to existing methods for training batch construction [9], [48], for the discernment of word-level semantics and the generalization capacity towards input expressions, we employ the most similar expressions as negative samples to increase the difficulty of contrastive learning. Concretely, in each training batch, for any object

$O_i, i \in \{1, 2, \dots, N_O\}$ in a video frame v , we randomly sample two sets of expressions from different modalities but sharing the same description for the same referred object, denoted as $\langle T_{i,j_1}, A_{i,k_1} \rangle$ and $\langle T_{i,j_2}, A_{i,k_2} \rangle$, where $j_1, j_2 \in \{1, 2, \dots, N_T\}$ and $k_1, k_2 \in \{1, 2, \dots, N_A\}$. The remaining part of the batch involves randomly selecting other video frames and corresponding two sets of text and audio.

In this mechanism, the positive samples for one modality in each batch consist of the same semantic representation in another, referring to the same object in the same video frame. The negative samples encompass not only the expressions from another modality of different video frames but also different semantic representations referring to the same object in the same video frame. To correctly discriminate between positive and negative samples, the model needs to enhance its feature extraction capability and attentively focus on the specific descriptive words conveyed in the expressions.

During the batch mentioned above, the number of samples for one modality of expression is denoted as N . First, we project the audio features $\mathcal{F}_{a,i}$ from the audio encoder and the text features $\mathcal{F}_{t,i}, i \in \{1, 2, \dots, N\}$ from the text encoder into a multi-modal embedding space using a linear mapping layer, denoted as follows:

$$\begin{aligned}\mathcal{E}_{t,i} &= \text{MLP}(\text{Avg}(\mathcal{F}_{t,i})), \\ \mathcal{E}_{a,i} &= \text{MLP}(\text{Avg}(\mathcal{F}_{a,i})),\end{aligned}\tag{1}$$

where $\text{MLP}(\cdot)$ denotes a multi-layer perceptron comprising two linear layers and one ReLU activation function. $\text{Avg}(\cdot)$ denotes average pooling. $\mathcal{E}_{t,i} \in \mathbb{R}^C$ and $\mathcal{E}_{a,i} \in \mathbb{R}^C$ represent the obtained multi-modal embeddings, both having the same dimensionality C . Inspired by [48], [49], our expression contrastive loss is defined as follows:

$$\begin{aligned}\ell_{\text{expr}} &= \frac{1}{2N} \sum_{i=1}^N \left[\log \frac{\exp(\frac{1}{\tau} \text{Sim}(\mathcal{E}_{a,i}, \mathcal{E}_{t,i}))}{\sum_{j=1}^N \exp(\frac{1}{\tau} \text{Sim}(\mathcal{E}_{a,i}, \mathcal{E}_{t,j}))} \right. \\ &\quad \left. + \log \frac{\exp(\frac{1}{\tau} \text{Sim}(\mathcal{E}_{t,i}, \mathcal{E}_{a,i}))}{\sum_{j=1}^N \exp(\frac{1}{\tau} \text{Sim}(\mathcal{E}_{t,i}, \mathcal{E}_{a,j}))} \right].\end{aligned}\tag{2}$$

where τ denotes the temperature constant and $\text{Sim}(\cdot)$ represents the cosine similarity function. This loss function compels one modality expression in the representation space to be closer to another with the same semantic content that refers to the same object in the video frame while being farther away from another modality expression with other semantic content.

Expression as Query. After the operations above, in the multi-modal embedding space, the audio embeddings \mathcal{E}_a can be determined best to match the text embeddings \mathcal{E}_t through the cosine similarity function and vice versa. Unlike the query generation paradigm proposed in [23], the Expression as Query (EQ) strategy is proposed to incorporate these embeddings into the original input query embeddings of the transformer decoder. In this manner, even when the decoder receives uni-modal queries, the aligned embeddings, which can approximately represent information from another modality, provide complementary support for predicting more accurate object masks in the decision space.

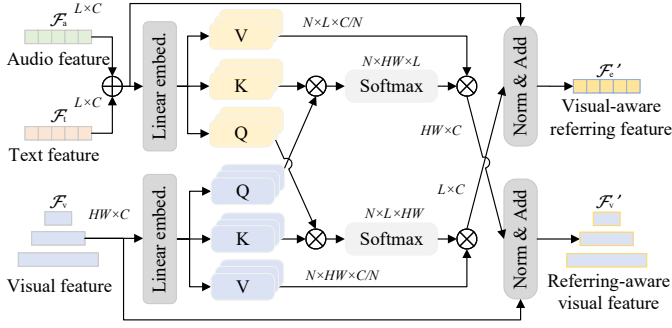


Fig. 3. The architecture of the proposed Expression-Visual Interaction (EVI) module. The text, audio, and visual features are obtained through their respective encoders. The visual-aware referring feature and referring-aware visual feature are fed into the segmentation network.

D. Multi-modal Interaction

As aforementioned, most previous text-guided or audio-guided networks [1], [3], [9], [23] concentrate on establishing relationships between video and single modality referring expression. Due to the inflexibility of text interactions in specific scenarios and the noise factors in speech interactions, these methods encounter limitations when deployed in practical applications. To address this issue, we propose designing a unified video segmentation model for audio and text-referring expressions. Inspired by the spirits of previous works [1], [23], [41], [50], we acknowledge that deep multi-modal fusion and interaction are crucial for developing a performant referring expression model.

As illustrated in Fig. 2, we further propose a multi-modal interaction module, named Expression-Visual Attention (EVA), designed to facilitate effective interactions among three modalities: audio, text, and vision. This module comprises two parallel streams, as depicted in Fig. 3 and Fig. 4, denoted as Expression-Visual Interaction (EVI) and Audio-Text Collaboration (ATC), respectively. EVI aims to establish effective interactions between auditory and textual cues with visual features, thereby emphasizing the matching visual regions and crucial cue elements. ATC exploits the complementarity between the two referring modalities of audio and text, refining one modality feature concerning another and vice versa.

Expression-Visual Interaction. As illustrated in Fig. 3, initially, given the visual feature $F_v \in \mathbb{R}^{C \times L_v}$ of the current frame, the acoustic feature $F_a \in \mathbb{R}^{C \times L}$ of the speech and the linguistic feature $F_t \in \mathbb{R}^{C \times L}$ of the sentence, we perform a linear combination between F_a and F_t to obtain the blended representation of the referring cues, denoted as F_e :

$$F_e = F_a + F_t, \quad (3)$$

In this way, both modalities can be placed in an equal position. In cases where only one modality expression is available, we initialize the other modality with zero vectors of matching dimension. Consequently, referring features F_e reduces to a single referring modality. This linearly decoupled property allows the model to process a single modality-referring expression independently.

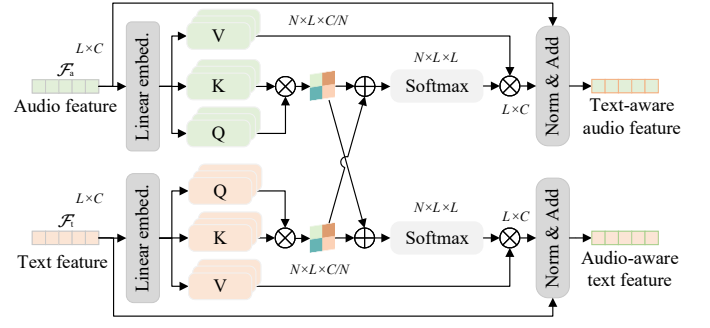


Fig. 4. The architecture of the proposed Audio-Text Collaboration (ATC) module. By employing ATC, the model exploits the complementarity between text and audio features, thus facilitating the extraction of pivotal expression features.

Afterward, inspired by [50]–[52], a multi-head cross-attention mechanism is employed to facilitate interaction between the referring features and visual features. Exactly, our method enables concurrent calculation of attention between text and visual, as well as between audio and visual, depicted as follows:

$$\begin{aligned} F_{v2e} &= \text{Softmax}\left(\frac{F_v W_v (F_e W_e)^T}{\sqrt{d_k}}\right) (F_e W_e^v)^T, \\ F_{e2v} &= \text{Softmax}\left(\frac{F_e W_e (F_v W_v)^T}{\sqrt{d_k}}\right) (F_v W_v^v)^T, \end{aligned} \quad (4)$$

where W_v , W_e , W_v^v , and W_e^v are learnable linear projection matrices for both features following [51]. After the cross-modal interaction, we perform a residual operation between raw features and obtained features:

$$\begin{aligned} F'_v &= F_v + F_{v2e}, \\ F'_e &= F_e + F_{e2v}. \end{aligned} \quad (5)$$

As a result, the visual features gain referring awareness, and the referring features acquire visual awareness. In particular, when there is only a single referring expression input, either $F_e = F_a$ or $F_e = F_t$. By employing fixed referring expression linear projection matrices W_e and W_e^v , the proposed model can seamlessly handle either the audio or text referring modality. Furthermore, this mixed-modal cross-attention mechanism serves two main purposes: (1) effectively capturing the common aspects of A-VOS and R-VOS tasks, resulting in a more generalized ability for video object segmentation according to referring expressions, and (2) alleviating overfitting when the model is in a single referring modality.

Audio-Text Collaboration. As illustrated in Fig. 4, the acoustic feature $F_a \in \mathbb{R}^{C \times L}$ of the speech and the linguistic feature $F_t \in \mathbb{R}^{C \times L}$ of the sentence are given. We perform a linear embedding to project the features and a multiplication for each modality to obtain attention matrices A_t and A_a independently, specifically:

$$\begin{aligned} A_a &= \frac{F_a W_a^q (F_t W_t^k)^T}{\sqrt{d_k}}, \\ A_t &= \frac{F_t W_t^q (F_a W_a^k)^T}{\sqrt{d_k}}, \end{aligned} \quad (6)$$

where W_a^q , W_a^k , W_t^q , and W_t^k are the learnable linear projection matrices for the features of each modality. After that, we perform an addition between A_a and A_t to obtain a shared attention matrix A_e :

$$A_e = A_a + A_t, \quad (7)$$

By utilizing shared attention calculations, we can obtain self-attention matrices for both the speech and text modalities, enabling their mutual complementary interaction. The shared attention matrix A_e is then used to reform an audio feature \mathcal{F}_a' and a text feature \mathcal{F}_t' :

$$\begin{aligned} \mathcal{F}_a' &= \text{Softmax}(A_{at})(\mathcal{F}_a W_v^v)^T, \\ \mathcal{F}_t' &= \text{Softmax}(A_{at})(\mathcal{F}_t W_t^v)^T, \end{aligned} \quad (8)$$

where W_a^v and W_t^v are learnable linear projection matrices for the features of the corresponding modality.

Finally, we concatenate the referring features from both branches as the output:

$$\mathcal{F}_r' = \mathcal{F}_e' + \mathcal{F}_a' + \mathcal{F}_t'. \quad (9)$$

Similar to EVI, when there is only a single referring modality input, either $A_e = A_a$ or $A_e = A_t$. Consequently, ATC can still function effectively under single-modality input scenarios. In contrast to the self-attention mechanism [51], the attention weight matrix of ATC is jointly learned from both referring modalities. This facilitates effective exploitation of the complementarity between audio and text and enhances the capacity to extract key information from the prompting expressions.

E. Segmentation and Optimization

Segmentation Transformer. Following [3], [23], [24], [41], the advanced transformer is adopted as the fundamental framework for video segmentation. Following [41], [50], [53], the contrastive learning loss is employed to associate each frame with the instance objects proposed by SimOTA [54]. During the inference phase, we apply Non-Maximum Suppression (NMS) to suppress redundant candidate targets. To distinguish between referred and non-referred objects, we compute the instance-referred matching scores, denoted as S_{ref} , by calculating the dot product between the instance features \mathcal{F}_{ins}' obtained from the decoder's output and the referring features \mathcal{F}_r' after average pooling, i.e., $S_{ref} = \mathcal{F}_{ins}' \text{Avg}(\mathcal{F}_r')^T$. Following [23], [41], to predict high-quality masks, a dynamic convolution-based mask head [55] is adopted.

Multi-Task Training. To endow the model with the knowledge of tackling R-VOS and A-VOS concurrently during training, we propose a novel approach for multi-task joint training of both tasks. First, We sample pairs of referring expressions with the same semantic meaning while exhibiting different modalities. Afterward, we input the encoded alignment features between text and audio cues into the network. Meanwhile, to avoid overfitting due to both modalities are available, we employ an equal probability dropout on either the text or audio features. Therefore, during training, the model encounters the three tasks with equal probability: text-guided segmentation, audio-guided segmentation, and segmentation guided by both text and audio.

Loss functions. Following previous works [20], [41], we adopt Focal [56], ℓ_1 & GIoU, contrastive [53], and the proposed expression contrastive losses as the matching (ℓ_{ref}), instance bounding box (ℓ_{box}), across frames contrastive (ℓ_{emb}), and expression contrastive (ℓ_{expr}) losses, respectively. Furthermore, drawing inspiration from [57], we integrate Adaptive Focal Loss and Dice Loss [58] to compute the mask loss ℓ_{mask} , which contributes to the prediction of referred object masks. Overall, we adopt the following loss functions to supervise our proposed model in an end-to-end manner:

$$\begin{aligned} \ell &= \lambda_{ref} \ell_{ref} + \lambda_{box} \ell_{box} + \lambda_{mask} \ell_{mask} \\ &\quad + \lambda_{emb} \ell_{emb} + \lambda_{expr} \ell_{expr}, \end{aligned} \quad (10)$$

where λ_{ref} , λ_{box} , λ_{mask} , λ_{emb} , and λ_{expr} are loss weights.

IV. EXPERIMENTS

A. Datasets

We conduct experiments on three datasets for R-VOS and four datasets for A-VOS, detailed as follows:

- 1) Ref-Youtube-VOS [16]: It is a large-scale dataset tailored for R-VOS. It encompasses 3,673 videos with 15K text clues for training and validation.
- 2) A2D-Sentences [2]: This dataset is created by augmenting the original A2D dataset [59] with additional textual expression. It comprises 3,754 videos with a collection of 6,655 sentences.
- 3) J-HMDB-Sentences [2]: It is an expansion of the original J-HMDB dataset [60], similar to A2D-Sentences. It contains 928 videos and their corresponding descriptions.
- 4) Audio-Guided-VOS [1]: Tailored for A-VOS, this dataset is an extension that complements Ref-Youtube-VOS, A2D-Sentences, and JHMDB-Sentences with additional 18,811 audio descriptions corresponding to the existing text.
- 5) A-Youtube-VOS [1]: This dataset is a part of Audio-Guided-VOS, encompassing a total of 11,226 audio clues. Following [1], the training set of Ref-Youtube-VOS is divided for building this dataset.
- 6) A-A2D [1]: It is a part of Audio-Guided-VOS, including 6,656 audio clues. We denote this dataset as A-A2D to distinguish it from A2D-Sentences.
- 7) A-J-HMDB [1]: It is a part of Audio-Guided-VOS, including 928 audio expressions. We denote this dataset as A-J-HMDB to distinguish it from J-HMDB-Sentences.

B. Evaluation Metrics

Following previous works [1], [23], region similarity \mathcal{J} , contour accuracy \mathcal{F} and their average value $\mathcal{J} \& \mathcal{F}$ are employed to evaluate the methods on Ref-Youtube-VOS [16], Audio-Guided-VOS [1], A-Youtube-VOS [1], A-A2D [1], and A-J-HMDB [1]. We upload the predictions to challenge the official server for evaluation on Ref-Youtube-VOS. For A2D-Sentences [2] and J-HMDB-Sentences [2], the Overall IoU, Mean IoU, and Precision@K, where $K \in [0.5, 0.6, 0.7, 0.8, 0.9]$, are adopted as the evaluation metrics.

TABLE I

COMPARISON IN $\mathcal{J}\&\mathcal{F}$, \mathcal{J} , AND \mathcal{F} BETWEEN EPCFORMER AND STATE-OF-THE-ART METHODS ON AUDIO-GUIDED-VOS [1], A-YOUTUBE-VOS [1], A-A2D [1], AND A-J-HMDB [1]. A-J-HMDB [1] IS ONLY USED TO EVALUATE THE CHECKPOINT TRAINED ON A-A2D [1]. THE BEST RESULTS ARE MARKED IN **BOLD**, AND THE SECOND-BEST RESULTS ARE UNDERLINED. +MEANS THAT THE RESULTS COME FROM [1].

Method	Backbone	Audio-Guided-VOS			A-Youtube-VOS			A-A2D			A-J-HMDB		
		$\mathcal{J}\&\mathcal{F}$	\mathcal{J}	\mathcal{F}	$\mathcal{J}\&\mathcal{F}$	\mathcal{J}	\mathcal{F}	$\mathcal{J}\&\mathcal{F}$	\mathcal{J}	\mathcal{F}	$\mathcal{J}\&\mathcal{F}$	\mathcal{J}	\mathcal{F}
URVOS+ [16] ECCV2020	ResNet-50	38.2	37.1	39.2	-	-	-	-	-	-	-	-	-
RAM+ [17] IJCAI2020	I3D	38.8	38.6	38.9	-	-	-	-	-	-	-	-	-
VisTR+ [22] CVPR2021	ResNet-50	38.8	38.0	39.5	-	-	-	-	-	-	-	-	-
Wnet [1] CVPR2022	ResNet-50	44.0	43.0	45.0	43.6	43.0	44.1	52.5	49.8	55.1	61.2	65.6	56.7
EPCFormer (ours)	ResNet-50	<u>54.3</u>	<u>54.3</u>	<u>54.2</u>	<u>53.7</u>	<u>52.4</u>	<u>55.0</u>	<u>63.0</u>	<u>60.7</u>	<u>65.2</u>	<u>62.6</u>	<u>67.4</u>	<u>57.9</u>
EPCFormer (ours)	ViT-H	59.0	58.9	59.1	56.7	55.0	58.5	64.9	62.6	67.3	63.7	68.5	58.8

TABLE II

COMPARISON IN PRECISION@K, OVERALL IOU, AND MEAN IOU BETWEEN EPCFORMER AND STATE-OF-THE-ART METHODS ON A2D-SENTENCES [2].

Method	Backbone	Precision					IoU		mAP
		P@0.5	P@0.6	P@0.7	P@0.8	P@0.9	Overall	Mean	
ACAN [10] ICCV2019	I3D	55.7	45.9	31.9	16.0	2.0	60.1	49.0	27.4
CMSA + CFSA [18] TPAMI2021	ResNet-101	48.7	43.1	35.8	23.1	5.2	61.8	43.2	-
CSTM [61] CVPR2021	I3D	65.4	58.9	49.7	33.3	9.1	66.2	56.1	39.9
CMPC-V [62] TPAMI2021	I3D	65.5	59.2	50.6	34.2	9.8	65.3	57.3	<u>40.4</u>
ClawCraneNet [63] Arxiv2021	ResNet-50	70.4	67.7	61.7	48.9	17.1	63.1	59.9	-
EPCFormer (ours)	ResNet-50	80.2	78.1	72.1	56.4	20.7	74.6	67.9	51.7
MTTR [3] CVPR2022	Video-Swin-T	75.4	71.2	63.8	48.5	16.9	72.0	64.0	46.1
ReferFormer [23] CVPR2022	Video-Swin-T	82.8	79.2	72.3	55.3	19.3	77.6	69.6	52.8
ReferFormer [23] CVPR2022	Video-Swin-B	83.1	80.4	74.1	57.9	21.2	78.6	70.3	55.0
DMFormer [4] TCSVT2023	Swin-T	81.3	78.8	71.9	55.2	20.3	76.0	68.3	54.3
DMFormer [4] TCSVT2023	Swin-L	83.7	81.8	75.7	60.0	24.3	78.4	70.9	<u>58.2</u>
OnlineRefer [24] ICCV2023	Video-Swin-B	83.1	80.2	73.4	56.8	21.7	79.6	70.5	-
SgMg [64] ICCV2023	Video-Swin-B	-	-	-	-	-	78.0	70.4	56.1
SgMg [64] ICCV2023	Video-Swin-T	-	-	-	-	-	79.9	72.0	58.5
EPCFormer (ours)	ViT-H	84.6	83.5	78.8	66.0	28.1	80.6	72.6	<u>58.2</u>

TABLE III

COMPARISON IN PRECISION@K, OVERALL IOU, AND MEAN IOU BETWEEN EPCFORMER AND STATE-OF-THE-ART METHODS ON J-HMDB-SENTENCES [2].

Method	Backbone	Precision					IoU		mAP
		P@0.5	P@0.6	P@0.7	P@0.8	P@0.9	Overall	Mean	
ACAN [10] ICCV2019	I3D	75.6	56.4	28.7	3.4	0.0	57.6	58.4	28.9
CMSA + CFSA [18] TPAMI2021	ResNet-101	76.4	62.5	38.9	9.0	0.1	62.8	58.1	-
CSTM [61] CVPR2021	I3D	78.3	63.9	37.8	7.6	0.0	59.8	60.4	33.5
CMPC-V [62] TPAMI2021	I3D	81.3	65.7	37.1	7.0	0.0	61.6	61.7	<u>34.2</u>
ClawCraneNet [63]	ResNet-50	88.0	79.6	56.6	14.7	0.2	64.4	65.6	-
EPCFormer (ours)	ResNet-50	94.8	89.1	66.7	18.9	0.0	71.1	70.7	42.8
MTTR [3] CVPR2022	Video-Swin-T	93.9	85.2	61.6	16.6	0.1	70.1	69.8	39.2
ReferFormer [23] CVPR2022	Video-Swin-T	95.8	89.3	66.8	18.9	0.2	71.9	71.0	42.2
ReferFormer [23] CVPR2022	Video-Swin-B	96.2	90.2	70.2	21.0	0.3	73.0	71.8	43.0
DMFormer [4] TCSVT2023	Swin-T	95.2	88.5	66.4	20.1	0.3	71.9	70.5	42.5
DMFormer [4] TCSVT2023	Swin-L	97.2	92.5	72.1	23.4	0.3	73.9	72.8	44.7
OnlineRefer [24] ICCV2023	Video-Swin-B	96.1	90.4	71.0	21.9	<u>0.2</u>	<u>73.5</u>	71.9	-
SgMg [64] ICCV2023	Video-Swin-B	-	-	-	-	-	72.8	71.7	44.4
SgMg [64] ICCV2023	Video-Swin-T	-	-	-	-	-	73.7	72.5	<u>45.0</u>
EPCFormer (ours)	ViT-H	97.6	93.1	72.6	<u>23.0</u>	0.0	74.0	73.1	45.5

C. Implementation Details

This work implements the proposed method with a frozen BERT-base [46] and an unfrozen HuBERT-Base [15]. Following [21], the transformer encoder and decoder are configured with 6 layers. The number of the transformer decoder's queries is set to 900. Following [41], we randomly sample 2 frames during training and only 1 frame during inference. The AdamW optimizer [65] is adopted with a base learning

rate of 10^{-4} and weight decay of 0.05. The model is trained on two A6000 GPUs of 48G RAM, with a batch size of 2 and 2 pairs of frames per GPU. Following [23], [24], for a fair comparison, our models are initialized by pre-trained weights from [41]. Additionally, we conduct joint training for 150,000 iterations on the Ref-Youtube-VOS and A-Youtube-VOS with the shared portion of the training set, 50,000 iterations on the A2D-Sentences [2] and A-A2D [1], and 150,000 iterations on Audio-Guided-VOS [1].

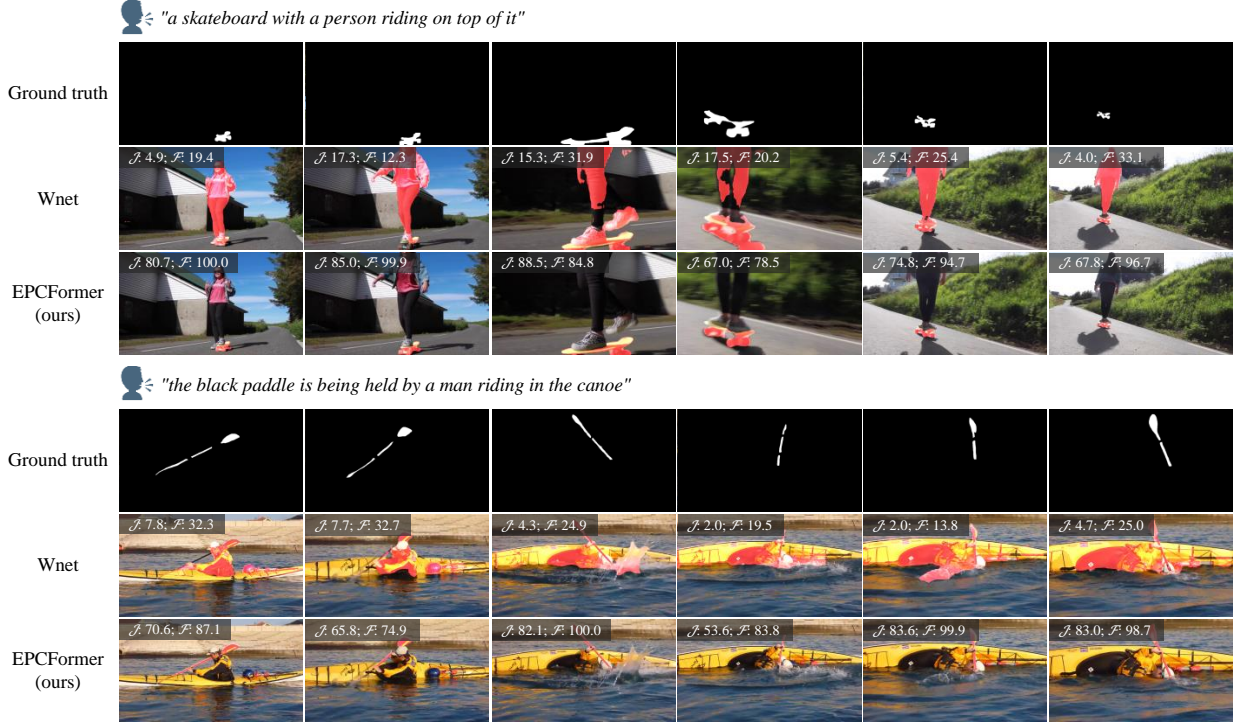


Fig. 5. Segmentation results of the proposed EPCFormer and Wnet [1] on A-YouTube-VOS [1]. The segmentation maps are superimposed in orange color over the original images. EPCFormer exhibits comprehensive exploitation of audio expressions, resulting in accurate localization and precise segmentation of referred objects.

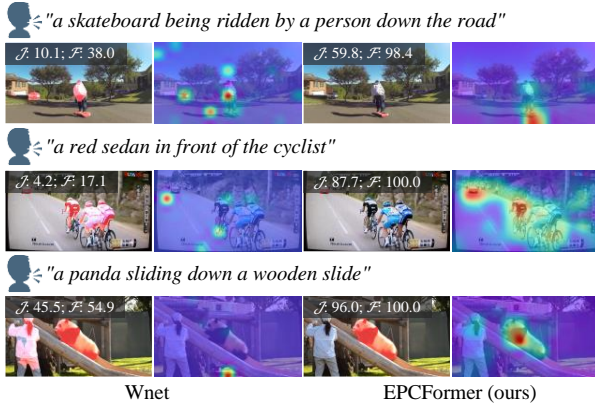


Fig. 6. Visualization of activation maps in the proposed EPCFormer and Wnet [1] on A-YouTube-VOS [1]. EPCFormer demonstrates the capability to discern referred objects based on audio expressions.

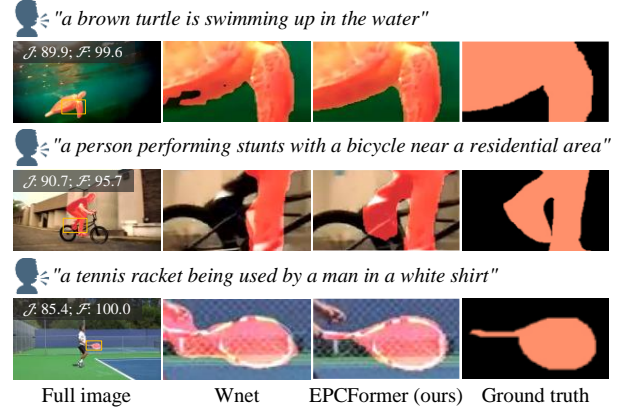


Fig. 7. The quality results in EPCFormer and Wnet [1] on A-YouTube-VOS [1]. The proposed EPCFormer can generate more detailed masks.

D. Comparison Methods

A wide variety of state-of-the-art A-VOS and R-VOS methods are incorporated for comparison:

1) A-VOS methods: The comparison A-VOS methods include Wnet [1], URVOS+ [16], RAM+ [17], and VisTR+ [22].

2) R-VOS methods: The R-VOS methods include CMPC-V [62], URVOS [16], YOFO [66], LBDT [19], MLSA [67], VLT [9], MTTR [3], ReferFormer [23], DMFormer [4], OnlineRefer [24], SgMg [64], ACAN [10], CMSA + CFSA [18], CSTM [61], CMPC-V [62], and ClawCraneNet [63].

E. Comparison with State-of-the-art A-VOS Methods

TABLE I lists the results of different A-VOS methods on four datasets. The results show that the proposed method achieves state-of-the-art performance across all datasets in various scenarios and with different types of targets. This is attributed to effectively establishing interactions and complementarity between multiple modalities. The following obvious findings can be observed: 1) Compared with the off-the-shelf methods using CNN as the backbone, the proposed EPCFormer, a ResNet-50 [44] backbone, achieves the overall J & F of 54.3%, 53.7%, 63.0%, and 62.6% on Audio-Guided-VOS [1], A-YouTube-VOS [1], A-A2D [1], and A-J-



Fig. 8. Segmentation results of EPCFormer and ReferFormer [23] on Ref-Youtube-VOS [16]. EPCFormer can more accurately locate specific targets and generate more detailed masks.

TABLE IV
COMPARISON IN $\mathcal{J} \& \mathcal{F}$, \mathcal{J} , AND \mathcal{F} BETWEEN EPCFORMER AND STATE-OF-THE-ART METHODS ON REF-YOUTUBE-VOS [16].

Method	Backbone	Ref-Youtube-VOS			
		$\mathcal{J} \& \mathcal{F}$	\mathcal{J}	\mathcal{F}	
CMPC-V [62]	TPAMI2021	I3D	47.5	45.6	49.3
URVOS [16]	ECCV2022	ResNet-50	47.2	45.3	49.2
YOFO [66]	AAAI2022	ResNet-50	48.6	47.5	49.7
LBDT [19]	CVPR2022	ResNet-50	49.4	48.2	50.6
MLSA [67]	CVPR2022	ResNet-50	<u>49.7</u>	48.4	51.0
ReferFormer [23]	CVPR2022	ResNet-50	55.6	54.8	<u>56.5</u>
EPCFormer (ours)	ResNet-50	55.6	<u>53.9</u>	57.2	
MTTR [3]	CVPR2022	Video-Swin-T	55.3	54.0	56.6
VLT [9]	TPAMI2022	Video-Swin-B	63.8	61.9	65.6
ReferFormer [23]	CVPR2022	Swin-L	62.4	60.8	64.0
ReferFormer [23]	CVPR2022	Video-Swin-B	62.9	61.3	64.6
DMFormer [4]	TCSVT2023	Swin-T	61.4	60.1	62.7
DMFormer [4]	TCSVT2023	Swin-L	<u>64.9</u>	63.4	<u>66.5</u>
OnlineRefer [24]	ICCV2023	Video-Swin-B	62.9	61.0	64.7
OnlineRefer [24]	ICCV2023	Swin-L	63.5	61.6	65.5
SgMg [64]	ICCV2023	Video-Swin-T	62.0	60.4	63.5
EPCFormer (ours)	ViT-H	65.0	<u>62.9</u>	67.2	

TABLE V
COMPARISON IN $\mathcal{J} \& \mathcal{F}$, \mathcal{J} , AND \mathcal{F} BETWEEN EPCFORMER AND DIFFERENT ASR-BASED METHODS ON A-YOUTUBE-VOS [1].

Method	Backbone	Audio Encoder	A-Youtube-VOS		
			$\mathcal{J} \& \mathcal{F}$	\mathcal{J}	\mathcal{F}
Wnet [1]	ResNet-50	MFCC layer	43.6	43.0	44.1
Wnet+ [1]	ResNet-50	HuBERT	41.9	41.8	42.0
ReferFormer+ [23]	ResNet-50	HuBERT	<u>47.7</u>	<u>47.4</u>	<u>47.9</u>
ReferFormer++ [23]	ResNet-50	HuBERT+BERT	40.8	40.2	41.4
EPCFormer (ours)	ResNet-50	HuBERT	53.7	52.4	55.0

HMDB [1], respectively, which are 10.3%, 10.1%, 11.5%, and 1.4% higher than the previous best solution Wnet [1]. 2) With a stronger ViT-Huge backbone [45], the proposed EPCFormer

further boosts the performance and achieves the overall $\mathcal{J} \& \mathcal{F}$ of 59.0%, 56.7%, 64.9%, and 63.7% on four different datasets, respectively. In addition, Fig. 5, Fig. 6, and Fig. 7 show the visualization results of EPCFormer and Wnet [1] on A-Youtube-VOS. Compared to the existing baseline, which struggles to localize targets accurately, the proposed EPCFormer exhibits greater robustness and exceptional accuracy when handling complex audio expressions, resulting in a more precise mask.

F. Comparison with State-of-the-art R-VOS Methods

TABLE II, TABLE III, and TABLE IV list results of different R-VOS methods on A2D-Sentences [2], J-HMDB-Sentences [2] and Ref-Youtube-VOS [16], respectively. The results show the performance of the proposed EPCFormer is competitive. The reason behind this lies in the introduced alignment and well-exploited complementarity between audio and text, which leads to the localization of crucial information in the text. In summary, the following observations lead to the conclusions: 1) As shown in TABLE II, EPCFormer leads to a higher mAP of 51.7% compared with other methods using CNNs as the backbone on A2D-Sentences. When compared with the methods using a transformer as the backbone, EPCFormer surpasses the nearest competitor SgMg [64] by 0.7% in Overall IoU and 0.6% in Mean IoU. 2) In TABLE III, with a ResNet-50 backbone [44], EPCFormer leads to a higher mAP of 42.8% on J-HMDB-Sentences, Compared with the most advanced SgMg [64] with the Video-Swin-T [68], EPCFormer with the ViT-Huge backbone [45] brings an improvement of 0.5% in mAP. (3) As shown in TABLE IV, EPCFormer using a CNN as the backbone outperforms the previous state-of-the-art method ReferFormer [23] in terms of \mathcal{F} on Ref-Youtube-VOS. When using a larger backbone, the performance of EPCFormer further boosts to overall $\mathcal{J} \& \mathcal{F}$ of 65.0%, outperforming the strong contender DMFormer [4] by 0.1%. Additionally, Fig. 8 visually demonstrates the improved mask segmentation quality of our proposed EPCFormer.

TABLE VI
ABLATION STUDIES BY USING OR NOT USING EVA, ECL, AND EQ ON
REF-YOUTUBE-VOS [16] AND A-YOUTUBE-VOS [1] DATASETS.

EVA	EA	EQ	Ref-Youtube-VOS			A-Youtube-VOS		
			$\mathcal{J}\&\mathcal{F}$	\mathcal{J}	\mathcal{F}	$\mathcal{J}\&\mathcal{F}$	\mathcal{J}	\mathcal{F}
✓	✓	✓	53.7	52.2	55.1	50.6	49.5	51.6
			54.6	53.1	56.1	52.4	51.3	53.4
			55.2	53.5	56.8	52.0	51.0	53.0
✓	✓	✓	54.8	53.4	56.2	52.2	51.4	53.1
			55.0	53.5	56.5	53.1	51.9	54.2
			54.9	53.3	56.4	52.4	51.3	53.5
✓	✓	✓	55.1	53.7	56.6	52.8	51.6	54.0
			55.6	53.9	57.2	53.7	52.4	55.0

TABLE VII
THE RESULT OF $\mathcal{J}\&\mathcal{F}$, \mathcal{J} AND \mathcal{F} UNDER DIFFERENT INTERACTION OF
EVA ON EPCFORMER. \leftrightarrow MEANS THE ATTENTION MATRIX OF ATC IS
NOT SHARED. \leftarrow AND \rightarrow MEANS THE ATTENTION MATRIX OF ATC IS
ONE-WAY SHARED. \leftrightarrow MEANS THE ATTENTION MATRIX OF ATC IS BI-WAY
SHARED.

Method	Ref-Youtube-VOS			A-Youtube-VOS		
	$\mathcal{J}\&\mathcal{F}$	\mathcal{J}	\mathcal{F}	$\mathcal{J}\&\mathcal{F}$	\mathcal{J}	\mathcal{F}
Text \leftrightarrow Audio	54.1	52.8	55.5	51.2	50.2	52.2
Text \leftarrow Audio	54.7	53.1	56.2	51.3	50.2	52.4
Text \rightarrow Audio	54.3	52.8	55.9	53.0	51.8	54.3
Text \leftrightarrow Audio	55.6	53.9	57.2	53.7	52.4	55.0

TABLE VIII
THE RESULT OF $\mathcal{J}\&\mathcal{F}$, \mathcal{J} AND \mathcal{F} UNDER DIFFERENT EQ SETTINGS ON
EPCFORMER. NOTE THAT TEXT&AUDIO MEANS TO USE BOTH TEXT AND
AUDIO EMBEDDINGS AS DECODER QUERIES.

Method	Ref-Youtube-VOS			A-Youtube-VOS		
	$\mathcal{J}\&\mathcal{F}$	\mathcal{J}	\mathcal{F}	$\mathcal{J}\&\mathcal{F}$	\mathcal{J}	\mathcal{F}
Text	55.5	53.6	57.3	53.0	51.8	54.1
Audio	54.9	53.3	56.4	53.6	52.4	54.7
Text&Audio	55.6	53.9	57.2	53.7	52.4	55.0

G. Comparison with ASR-based Methods

To investigate the impact of different ASR integration approaches, we established several groups of baselines based on representative existing methods, detailed as follows:

1) Wnet+ [1]: This is the extension of Wnet [1], where the MFCC layer [47] is replaced with a HuBERT-Base [15] as the audio encoder.

2) ReferFormer+ [23]: To adapt to A-VOS, this is the extension of [23] where the original text encoder is replaced with a HuBERT-Base [15] as the audio encoder.

3) ReferFormer++ [23]: This is the augmentation of [23] with an additional HuBERT-Base [15] as the ASR pre-processing for raw audio transcriptions.

TABLE V lists the performances of EPCFormer and the above methods on A-Youtube-VOS [1]. It can be seen from TABLE V that our method achieves superior results in terms of $\mathcal{J}\&\mathcal{F}$, \mathcal{J} , and \mathcal{F} . The primary reason is that the proposed EPCFormer effectively taps into the full potential of pre-trained ASR models. For example, compared with Wnet+ [1] and ReferFormer+ [23], our EPCFormer achieves at least 10.6% and 5.0% improvements and at most 13.0% and

7.1% on three evaluation metrics, respectively. Compared with ReferFormer++ [23] using an ASR model first, the proposed EPCFormer is 12.9% higher than it at the overall $\mathcal{J}\&\mathcal{F}$. Furthermore, when compared with the original Wnet [1], Wnet+ [1] using a HuBERT-Base [15] as an audio encoder is defeated. It indicates that the performance improvement requires a powerful feature encoding and relies on a more robust cross-modal interaction mechanism.

H. Ablation Studies

Analysis of the Proposed Components. TABLE VI presents the ablation results of the proposed modules, where we remove the components of EVA, EA, and EQ as our baseline model. The obtained results demonstrate the effectiveness of our methods, as the overall performance is superior when all components are integrated. The reason lies in the positive roles played by the proposed modules, which facilitate interactions among text, audio, and visual modalities. This conclusion can be deduced from the following observations: 1) Compared with the baseline, incorporating EVA, EA, and EQ yields considerable enhancements of 0.9%, 1.5%, and 1.1% in terms of $\mathcal{J}\&\mathcal{F}$ on Ref-Youtube-VOS [16], while delivering enhancements of 1.8%, 1.4%, and 1.6% in $\mathcal{J}\&\mathcal{F}$ on A-Youtube-VOS [1], respectively. 2) From the fifth to the last row, the model's performance progressively improves as the modules are incorporated.

In addition, TABLE VII shows the impact of interactions between audio and text modalities on the ATC module in the EVA, where the optimal performance is achieved when both audio and text implement bidirectional interaction. As evidenced in TABLE VIII, the results showcase the positive impact of employing the EQ mechanism on the audio and text modalities, where the best results are obtained when both audio and text implement the EQ mechanism.

Analysis of Multi-task Training. TABLE IX shows the impact of various multi-task training on the performance of the proposed EPCFormer. We can observe the following evident findings from TABLE IX. First, when trained with only text expressions, the method's performance reaches 39.9% $\mathcal{J}\&\mathcal{F}$ on A-VOS, closely comparable to the outcomes achieved by existing methods. This demonstrates that EPCFormer, through learning from a single modality, not only achieves adequate fitting on one task alone but also attains a certain level of accuracy on the other task. This reflects the generality of the proposed method, where shared knowledge can be transferred across both tasks. Second, as evident from the last row, the model attains its peak performance when encountering an equiprobable combination of text, audio, and their simultaneous presence during the training stage. This indicates that the devised multi-task training effectively simultaneously stimulates the model's performance on both tasks.

I. Hyper-parameter Analysis

TABLE X and TABLE XI present the impact of different MLP layers and the contrast loss weight λ_{expr} on the proposed model, respectively. The results reveal that the model performs optimally with two MLP layers and $\lambda_{expr} = 1$. As illustrated

TABLE IX

THE RESULT OF $\mathcal{J}\&\mathcal{F}$, \mathcal{J} , AND \mathcal{F} UNDER DIFFERENT MULTI-TASK TRAINING SETTINGS ON EPCFORMER. TEXT, AUDIO, AND MIX REPRESENT TEXT, AUDIO, AND A COMBINATION OF TEXT&AUDIO ARE INPUT INTO THE NETWORK SIMULTANEOUSLY FOR TRAINING.

Audio	Text	Mix	Ref-Youtube-VOS			A-Youtube-VOS		
			$\mathcal{J}\&\mathcal{F}$	\mathcal{J}	\mathcal{F}	$\mathcal{J}\&\mathcal{F}$	\mathcal{J}	\mathcal{F}
✓			39.4	38.0	40.8	50.7	49.5	51.9
	✓		53.7	52.1	55.2	39.2	38.5	39.9
✓	✓		53.7	52.3	55.1	51.1	50.1	52.1
✓	✓	✓	55.6	53.9	57.2	53.7	52.4	55.0

TABLE X

THE RESULT OF $\mathcal{J}\&\mathcal{F}$, \mathcal{J} , AND \mathcal{F} UNDER THE DIFFERENT NUMBERS OF MLP LAYERS ON EPCFORMER.

Setting	Ref-Youtube-VOS			A-Youtube-VOS		
	$\mathcal{J}\&\mathcal{F}$	\mathcal{J}	\mathcal{F}	$\mathcal{J}\&\mathcal{F}$	\mathcal{J}	\mathcal{F}
1	54.6	53.2	56.1	53.4	52.3	54.5
2	55.6	53.9	57.2	53.7	52.4	55.0
3	54.7	53.1	56.2	53.2	52.1	54.3
4	55.2	53.7	56.8	53.6	52.4	54.7

TABLE XI

THE RESULT OF $\mathcal{J}\&\mathcal{F}$, \mathcal{J} , AND \mathcal{F} UNDER DIFFERENT VALUES OF THE LOSS WEIGHT λ_{expr} ON EPCFORMER.

λ_{expr}	Ref-Youtube-VOS			A-Youtube-VOS		
	$\mathcal{J}\&\mathcal{F}$	\mathcal{J}	\mathcal{F}	$\mathcal{J}\&\mathcal{F}$	\mathcal{J}	\mathcal{F}
0	54.7	53.2	56.2	52.4	51.3	53.5
0.5	54.6	53.1	56.1	53.5	52.5	54.4
1	55.6	53.9	57.2	53.7	52.4	55.0
1.5	55.0	53.4	56.6	53.1	52.1	54.2

in TABLE X, it is evident that augmenting the number of MLP layers from 1 to 2 results in enhanced performance in both tasks. However, when the number of layers reaches 3, the performance decline is observed. Upon comparing the model's performance for varying λ_{expr} weight values, *i.e.*, $\lambda_{expr} = 0, 0.5, 1, 1.5$, as shown in TABLE XI, it becomes apparent that $\lambda_{expr} = 1$ yields the most favorable outcomes.

V. CONCLUSION

In this paper, we propose an Expression Prompt Collaboration Transformer (EPCFormer) for universal referring video object segmentation. In our proposed method, both audio and text can be analyzed effectively to guide the segmentation of referred video objects. First, to achieve the alignment of semantically related audio and text, the Expression Alignment (EA) module based on contrastive learning is introduced, which provides supervision after the linear mapping of both modalities into a multi-modal embedding space. Then, to achieve comprehensive interaction and fusion among audio, text, and visual data for the precise generation of masks, the Expression-Visual Attention (EVA) mechanism is proposed. It further delves into the complementary relationship between text and audio. Extensive experimentation demonstrates that

our proposed method achieves state-of-the-art performance on R-VOS and A-VOS tasks by leveraging shared weights.

However, there are two limitations to the proposed EPCFormer: 1) In scenarios where numerous objects are present in the video, the methods might encounter challenges in accurately localizing the expressed objects due to insufficient expression analysis. Therefore, enhancing the network's expression analysis capability is imperative for improving the model's accuracy. 2) As the primary application scenario for our EPCFormer involves human-computer interaction, developing a lightweight network tailored for edge devices is promising to offer a more convenient mode of interaction. These leave space for further investigation in our future work.

ACKNOWLEDGMENT

This work is partially supported by the National Natural Science Foundation of China (No. U21A20518, No. 61976086, and 62106071), the Special Project of Foshan Science and Technology Innovation Team (No. FS0AA-KJ919-4402-0069), and in part by Hangzhou Surlmage Technology Company Ltd.

REFERENCES

- [1] W. Pan *et al.*, "Wnet: Audio-guided video object segmentation via wavelet-based cross-modal denoising networks," in *Proc. IEEE Conf. Comput. Vis. Pattern Recognit.*, 2022, pp. 1310–1321.
- [2] K. Gavriluk, A. Ghodrati, Z. Li, and C. G. M. Snoek, "Actor and action video segmentation from a sentence," in *Proc. IEEE Conf. Comput. Vis. Pattern Recognit.*, 2018, pp. 5958–5966.
- [3] A. Botach, E. Zheltonozhskii, and C. Baskin, "End-to-end referring video object segmentation with multimodal transformers," in *Proc. IEEE Conf. Comput. Vis. Pattern Recognit.*, 2022, pp. 4975–4985.
- [4] M. Gao, J. Yang, J. Han, K. Lu, F. Zheng, and G. Montana, "Decoupling multimodal transformers for referring video object segmentation," *IEEE Trans. Circuit Syst. Video Technol.*, 2023.
- [5] M. Sun, J. Xiao, E. G. Lim, C. Zhao, and Y. Zhao, "Unified multi-modality video object segmentation using reinforcement learning," *IEEE Trans. Circuit Syst. Video Technol.*, 2023.
- [6] H.-C. Shih, "A survey of content-aware video analysis for sports," *IEEE Trans. Circuit Syst. Video Technol.*, vol. 28, no. 5, pp. 1212–1231, 2018.
- [7] Y. Ji, Y. Yang, F. Shen, H. T. Shen, and X. Li, "A survey of human action analysis in HRI applications," *IEEE Trans. Circuit Syst. Video Technol.*, vol. 30, no. 7, pp. 2114–2128, 2020.
- [8] F. Tang, Y. Wu, X. Hou, and H. Ling, "3D mapping and 6D pose computation for real time augmented reality on cylindrical objects," *IEEE Trans. Circuit Syst. Video Technol.*, vol. 30, no. 9, pp. 2887–2899, 2020.
- [9] H. Ding, C. Liu, S. Wang, and X. Jiang, "VLT: Vision-language transformer and query generation for referring segmentation," *IEEE Trans. Pattern Anal. Mach. Intell.*, vol. 45, no. 6, pp. 7900–7916, 2023.
- [10] H. Wang, C. Deng, J. Yan, and D. Tao, "Asymmetric cross-guided attention network for actor and action video segmentation from natural language query," in *Proc. IEEE Int. Conf. Comput. Vis.*, 2019, pp. 3938–3947.
- [11] A. Khoreva, A. Rohrbach, and B. Schiele, "Video object segmentation with language referring expressions," in *Proc. Asi. Conf. Comput. Vis.*, vol. 11364, 2018, pp. 123–141.
- [12] Y. Jing, T. Kong, W. Wang, L. Wang, L. Li, and T. Tan, "Locate then segment: A strong pipeline for referring image segmentation," in *Proc. IEEE Conf. Comput. Vis. Pattern Recognit.*, 2021, pp. 9858–9867.
- [13] J. Lin *et al.*, "BRPPNet: Balanced privacy protection network for referring personal image privacy protection," *Expert Syst. Appl.*, p. 120960, 2023.
- [14] S. Schneider, A. Baevski, R. Collobert, and M. Auli, "wav2vec: Un-supervised pre-training for speech recognition," *Proc. Annu. Conf. Int. Speech Commun. Assoc.*, pp. 3465–3469, 2019.
- [15] W.-N. Hsu, B. Bolte, Y.-H. H. Tsai, K. Lakhotia, R. Salakhutdinov, and A. Mohamed, "HuBERT: Self-supervised speech representation learning by masked prediction of hidden units," *IEEE/ACM Trans. Audio Speech Lang. Process.*, vol. 29, pp. 3451–3460, 2021.

- [16] S. Seo, J.-Y. Lee, and B. Han, "URVOS: Unified referring video object segmentation network with a large-scale benchmark," in *Proc. Eur. Conf. Comput. Vis.*, vol. 12360, 2020, pp. 208–223.
- [17] K. Ning, L. Xie, F. Wu, and Q. Tian, "Polar relative positional encoding for video-language segmentation," in *Proc. Int. Joint Conf. Artif. Intell.*, 2020, pp. 948–954.
- [18] L. Ye, M. Rochan, Z. Liu, X. Zhang, and Y. Wang, "Referring segmentation in images and videos with cross-modal self-attention network," *IEEE Trans. Pattern Anal. Mach. Intell.*, vol. 44, no. 7, pp. 3719–3732, 2022.
- [19] Z. Ding, T. Hui, J. Huang, X. Wei, J. Han, and S. Liu, "Language-bridged spatial-temporal interaction for referring video object segmentation," in *Proc. IEEE Conf. Comput. Vis. Pattern Recognit.*, 2022, pp. 4954–4963.
- [20] N. Carion, F. Massa, G. Synnaeve, N. Usunier, A. Kirillov, and S. Zagoruyko, "End-to-end object detection with transformers," in *Proc. Eur. Conf. Comput. Vis.*, vol. 12346, 2020, pp. 213–229.
- [21] X. Zhu, W. Su, L. Lu, B. Li, X. Wang, and J. Dai, "Deformable DETR: Deformable transformers for end-to-end object detection," in *Proc. Int. Conf. Learn. Represent.*, 2021.
- [22] Y. Wang *et al.*, "End-to-end video instance segmentation with transformers," in *Proc. IEEE Conf. Comput. Vis. Pattern Recognit.*, 2021, pp. 8741–8750.
- [23] J. Wu, Y. Jiang, P. Sun, Z. Yuan, and P. Luo, "Language as queries for referring video object segmentation," in *Proc. IEEE Conf. Comput. Vis. Pattern Recognit.*, 2022, pp. 4964–4974.
- [24] D. Wu, T. Wang, Y. Zhang, X. Zhang, and J. Shen, "OnlineRefer: A simple online baseline for referring video object segmentation," in *Proc. IEEE Int. Conf. Comput. Vis.*, 2023.
- [25] J. Zhou *et al.*, "Audio-visual segmentation," in *Proc. Eur. Conf. Comput. Vis.*, vol. 13697, 2022, pp. 386–403.
- [26] B. Cheng, I. Misra, A. G. Schwing, A. Kirillov, and R. Girdhar, "Masked-attention mask transformer for universal image segmentation," in *Proc. IEEE Conf. Comput. Vis. Pattern Recognit.*, 2022.
- [27] S. Gao, Z. Chen, G. Chen, W. Wang, and T. Lu, "AVSegFormer: Audio-visual segmentation with transformer," *arXiv preprint arXiv:2307.01146*, 2023.
- [28] J. Jain, J. Li, M. T. Chiu, A. Hassani, N. Orlov, and H. Shi, "OneFormer: One transformer to rule universal image segmentation," in *Proc. IEEE Conf. Comput. Vis. Pattern Recognit.*, 2023, pp. 2989–2998.
- [29] J. Zhang, H. Liu, K. Yang, X. Hu, R. Liu, and R. Stiefelhagen, "CMX: Cross-modal fusion for RGB-X semantic segmentation with transformers," *IEEE Trans. Intell. Transp. Syst.*, 2023.
- [30] J. Zhang *et al.*, "Delivering arbitrary-modal semantic segmentation," in *Proc. IEEE Conf. Comput. Vis. Pattern Recognit.*, 2023, pp. 1136–1147.
- [31] X. Gu *et al.*, "DaTaSeg: Taming a universal multi-dataset multi-task segmentation model," *arXiv preprint arXiv:2306.01736*, 2023.
- [32] X. Zhang, K. Yang, J. Lin, J. Yuan, Z. Li, and S. Li, "VPUFormer: Visual prompt unified transformer for interactive image segmentation," *arXiv preprint arXiv:2306.06656*, 2023.
- [33] X. Wang, X. Zhang, Y. Cao, W. Wang, C. Shen, and T. Huang, "SegGPT: Segmenting everything in context," in *Proc. IEEE Int. Conf. Comput. Vis.*, 2023.
- [34] A. Kolesnikov *et al.*, "Big transfer (BiT): General visual representation learning," in *Proc. Eur. Conf. Comput. Vis.*, vol. 12350, 2020, pp. 491–507.
- [35] T. Chen, S. Saxena, L. Li, T.-Y. Lin, D. J. Fleet, and G. E. Hinton, "A unified sequence interface for vision tasks," in *Proc. Adv. Neural Inform. Process. Syst.*, vol. 35, 2022, pp. 31 333–31 346.
- [36] W. Zhang, J. Pang, K. Chen, and C. C. Loy, "K-Net: Towards unified image segmentation," in *Proc. Adv. Neural Inform. Process. Syst.*, vol. 34, 2021, pp. 10 326–10 338.
- [37] B. Cheng, A. G. Schwing, and A. Kirillov, "Per-pixel classification is not all you need for semantic segmentation," in *Proc. Adv. Neural Inform. Process. Syst.*, vol. 34, 2021, pp. 17 864–17 875.
- [38] G. Luo *et al.*, "Multi-task collaborative network for joint referring expression comprehension and segmentation," in *Proc. IEEE Conf. Comput. Vis. Pattern Recognit.*, 2020, pp. 10031–10040.
- [39] F. Li *et al.*, "Mask DINO: Towards a unified transformer-based framework for object detection and segmentation," in *Proc. IEEE Conf. Comput. Vis. Pattern Recognit.*, 2023, pp. 3041–3050.
- [40] H. Zhang *et al.*, "A simple framework for open-vocabulary segmentation and detection," *arXiv preprint arXiv:2303.08131*, 2023.
- [41] B. Yan *et al.*, "Universal instance perception as object discovery and retrieval," in *Proc. IEEE Conf. Comput. Vis. Pattern Recognit.*, 2023, pp. 15 325–15 336.
- [42] A. Kirillov *et al.*, "Segment anything," in *Proc. IEEE Int. Conf. Comput. Vis.*, 2023.
- [43] X. Zou *et al.*, "Segment everything everywhere all at once," *arXiv preprint arXiv:2304.06718*, 2023.
- [44] K. He, X. Zhang, S. Ren, and J. Sun, "Deep residual learning for image recognition," in *Proc. IEEE Conf. Comput. Vis. Pattern Recognit.*, 2016, pp. 770–778.
- [45] A. Dosovitskiy *et al.*, "An image is worth 16x16 words: Transformers for image recognition at scale," in *Proc. Int. Conf. Learn. Represent.*, 2021.
- [46] J. Devlin, M.-W. Chang, K. Lee, and K. Toutanova, "BERT: Pre-training of deep bidirectional transformers for language understanding," in *Proc. Conf. North Amer. Chapter Assoc. Comput. Linguistics: Human Lang. Technol.*, vol. 1, 2019, pp. 4171–4186.
- [47] L. Bouchakour and M. Debyeche, "MFCCs and gabor features for improving continuous arabic speech recognition in mobile communication modified," in *Proc. Int. Conf. Adv. Aspects Softw. Eng.*, vol. 2326, 2018, pp. 115–121.
- [48] Y. Wu, K. Chen, T. Zhang, Y. Hui, T. Berg-Kirkpatrick, and S. Dubnov, "Large-scale contrastive language-audio pretraining with feature fusion and keyword-to-caption augmentation," in *Proc. IEEE Int. Conf. Acoust., Speech Signal Process.*, 2023, pp. 1–5.
- [49] A. Radford *et al.*, "Learning transferable visual models from natural language supervision," in *Proc. Int. Conf. Mach. Learn.*, vol. 139, 2021, pp. 8748–8763.
- [50] L. Li *et al.*, "Grounded language-image pre-training," in *Proc. IEEE Conf. Comput. Vis. Pattern Recognit.*, 2022, pp. 10955–10965.
- [51] A. Vaswani *et al.*, "Attention is all you need," in *Proc. Adv. Neural Inform. Process. Syst.*, vol. 30, 2017, pp. 5998–6008.
- [52] C. Liu, H. Ding, Y. Zhang, and X. Jiang, "Multi-modal mutual attention and iterative interaction for referring image segmentation," *IEEE Trans. Image Processing*, vol. 32, pp. 3054–3065, 2023.
- [53] J. Wu, Q. Liu, Y. Jiang, S. Bai, A. Yuille, and X. Bai, "In defense of online models for video instance segmentation," in *Proc. Eur. Conf. Comput. Vis.*, vol. 13688, 2022, pp. 588–605.
- [54] Z. Ge, S. Liu, F. Wang, Z. Li, and J. Sun, "YOLOX: Exceeding YOLO series in 2021," *arXiv preprint arXiv:2107.08430*, 2021.
- [55] Z. Tian, C. Shen, and H. Chen, "Conditional convolutions for instance segmentation," in *Proc. Eur. Conf. Comput. Vis.*, vol. 12346, 2020, pp. 282–298.
- [56] T.-Y. Lin, P. Goyal, R. Girshick, K. He, and P. Dollár, "Focal loss for dense object detection," in *Proc. IEEE Int. Conf. Comput. Vis.*, 2017, pp. 2999–3007.
- [57] J. Lin *et al.*, "AdaptiveClick: Clicks-aware transformer with adaptive focal loss for interactive image segmentation," *arXiv preprint arXiv:2305.04276*, 2023.
- [58] F. Milletari, N. Navab, and S.-A. Ahmadi, "V-Net: Fully convolutional neural networks for volumetric medical image segmentation," in *Proc. Int. Conf. 3D Vis.*, 2016, pp. 565–571.
- [59] C. Xu, S.-H. Hsieh, C. Xiong, and J. J. Corso, "Can humans fly? Action understanding with multiple classes of actors," in *Proc. IEEE Conf. Comput. Vis. Pattern Recognit.*, 2015, pp. 2264–2273.
- [60] H. Jhuang, J. Gall, S. Zuffi, C. Schmid, and M. J. Black, "Towards understanding action recognition," in *Proc. IEEE Int. Conf. Comput. Vis.*, 2013, pp. 3192–3199.
- [61] T. Hui *et al.*, "Collaborative spatial-temporal modeling for language-queried video actor segmentation," in *Proc. IEEE Conf. Comput. Vis. Pattern Recognit.*, 2021, pp. 4187–4196.
- [62] S. Liu, T. Hui, S. Huang, Y. Wei, B. Li, and G. Li, "Cross-modal progressive comprehension for referring segmentation," *IEEE Trans. Pattern Anal. Mach. Intell.*, pp. 4761–4775, 2022.
- [63] C. Liang, Y. Wu, Y. Luo, and Y. Yang, "ClawCraneNet: Leveraging object-level relation for text-based video segmentation," *arXiv preprint arXiv:2103.10702*, 2021.
- [64] B. Miao, M. Bennamoun, Y. Gao, and A. Mian, "Spectrum-guided multi-granularity referring video object segmentation," in *Proc. IEEE Int. Conf. Comput. Vis.*, 2023.
- [65] I. Loshchilov and F. Hutter, "Decoupled weight decay regularization," in *Proc. Int. Conf. Learn. Represent.*, 2019.
- [66] D. Li *et al.*, "You only infer once: Cross-modal meta-transfer for referring video object segmentation," in *Proc. AAAI Conf. Artif. Intell.*, vol. 36, no. 2, 2022, pp. 1297–1305.
- [67] D. Wu, X. Dong, L. Shao, and J. Shen, "Multi-level representation learning with semantic alignment for referring video object segmentation," in *Proc. IEEE Conf. Comput. Vis. Pattern Recognit.*, 2022, pp. 4986–4995.
- [68] Z. Liu *et al.*, "Video swin transformer," in *Proc. IEEE Conf. Comput. Vis. Pattern Recognit.*, 2022, pp. 3192–3201.